Chapter 11

Internal Waves and Instabilities

11.1 A two layer model for internal waves.

In the last chapter we considered gravity waves in a single fluid layer and discussed the frequency and wave number relation, e.g. the *dispersion relation*. Not surprisingly, we found that for each real wavenumber there was a real frequency. In this chapter we will take up the discussion of a fluid whose density is variable and when , as in the last chapter, we add the effect of a mean flow we will find situations in which for some real wavenumbers the resulting frequency for free waves is a complex number. We will have to interpret just what that means. We will find that in such cases we can consider the original, wave-free state as an unstable equilibrium o f the system that can become unstable and spontaneously generate waves. This spontaneous generation is the fundamental reason for the existence of fluid turbulence and its manifestations in the oceans and atmosphere from small scales to the large scales where eddies and synoptic scale disturbances occur. Although the physics of small scale and large scale instabilities differ, the overall approach to the question of the dynamics of instability is the same.

We begin by taking advantage of the relative simplicity of irrotational flow theory. That implies that we are considering scales small enough in space and fast enough in time so that the rotation of the Earth can be neglected. Consider the situation shown in Figure 11.1.1.

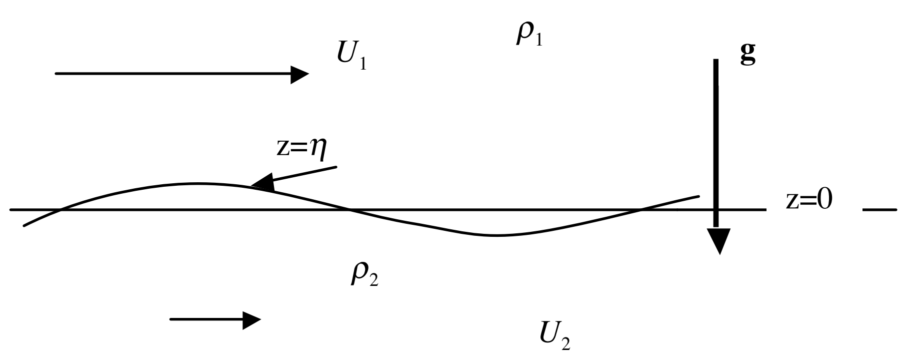

Figure 11.1.1 Two fluid layers of different densities and mean flows separated by an interface z=η.

Two fluids, each with constant but distinct densities are separated by an interface, originally at z =0. In each layer there is a mean flow, uniform in space and time flowing in the x direction. The speed of each of the flows may be distinct from one another. A perturbation is introduced into the system by perturbing the interface a small amount so that the interface departs from the z=0 surface by an amount $\eta(x,t)$. In each region the density is constant, friction is ignored as being negligible and in the absence of planetary rotation, motion started from rest will be, and remain, irrotational. Thus in each region above and below the interface,

$$\nabla^2\varphi_j = 0, \qquad j = 1,2 \tag{11.1.1}$$

where the index j is 1 for the region above the interface and equals 2 for the region below the interface. At the interface the Bernoulli equation in each fluid yields,

$$\frac{\partial\varphi_j}{\partial t} + \frac{1}{2}\left|\nabla\varphi_j\right|^2 + g\eta + \frac{p_j(x,\eta,t)}{\rho_j} = 0 \tag{11.1.2}$$

and the kinematic condition, applied on each side of the interface is,

$$\frac{\partial\eta}{\partial t} + \nabla\varphi_j \bullet \nabla\eta = \frac{\partial\varphi_j}{\partial z} \tag{11.1.3}$$

We consider small perturbations to the streaming motion in each layer and the linearized forms of (11.1.2) and (11.1.3) are, as in the last chapter,

$$\left(\frac{\partial}{\partial t} + U_j\frac{\partial}{\partial x}\right)\varphi_j + g\eta = -\frac{p_j}{\rho_j}$$

$$\left(\frac{\partial}{\partial t} + U_j\frac{\partial}{\partial x}\right)\eta = \frac{\partial\varphi_j}{\partial z} \tag{11.1.4 a, b}$$

and, as before, we can apply these boundary conditions on the undisturbed free surface position z=0. For simplicity, we consider the fluid regions each to be semi-infinite in the z direction. Using the results of the last chapter we recognize that this only means that if there are lateral boundaries they are much further away from the interface than a wavelength of the disturbance. A wave-like solution of Laplace's equation in each region that satisfies the condition that the disturbance be finite as $|z|$ becomes very large is,

$$\varphi_1 = \operatorname{Re} A_1 e^{i(kx-\omega t)} e^{-kz},$$

$$\varphi_2 = \operatorname{Re} A_2 e^{i(kx-\omega t)} e^{kz}, \qquad \text{(11.1.5, a, b, c)}$$

$$\eta = \operatorname{Re} N_o e^{i(kx-\omega t)}$$

Using (11.1.5) in the kinematic boundary conditions, yields,

$$i(Uk-\omega)N_o = -kA_1,$$

$$\text{(11.1.6 a, b)}$$

$$i(Uk-\omega)N_o = kA_2$$

or eliminating N_0,

$$\frac{A_1}{U_1 k-\omega} = -\frac{A_2}{U_2 k-\omega},$$

$$\text{(11.1.7 a. b)}$$

$$N_o = \frac{ik}{U_1 k-\omega} A_1$$

The dynamic boundary condition applied at the interface requires that the pressure be the same in each layer at the interface. Using the Bernoulli equation (11.1.4) we obtain,

$$-p_1 = \rho_1 g\eta + \rho_1\left(\frac{\partial}{\partial t} + U_1\frac{\partial}{\partial x}\right)\varphi_1 = \rho_2 g\eta + \rho_2\left(\frac{\partial}{\partial t} + U_2\frac{\partial}{\partial x}\right)\varphi_2 = -p_2 \qquad \text{(11.1.8)}$$

at z=0. Or,

$$\left(\rho_2-\rho_1\right)g\eta = \rho_1\left(\frac{\partial}{\partial t} + U_1\frac{\partial}{\partial x}\right)\varphi_1 - \rho_2\left(\frac{\partial}{\partial t} + U_2\frac{\partial}{\partial x}\right)\varphi_2 \qquad \text{(11.1.9)}$$

With the solutions for the velocity potentials and the interface, this leads to a second algebraic equation for A_1 and A_2, namely,

$$-\frac{(\rho_2-\rho_1)gk}{i(U_1k-\omega)}A_1 = i\rho_1\left(U_1k-\omega\right)A_1 - i\rho_2\left(U_2k-\omega\right)A_2 \qquad (11.1.10)$$

We can then use the kinematic condition (11.1.7a) to eliminate A_2 from (11.1.10) and obtain,

$$A_1\left[\left(\rho_2-\rho_1\right)gk-\rho_1\left(U_1k-\omega\right)^2-\rho_2\left(U_2k-\omega\right)^2\right]=0 \qquad (11.1.11)$$

If A_1 is not zero, i.e. if the disturbance is not trivial, then the quantity in the square bracket must vanish. This yield a quadratic equation for ω in terms of k and the parameters of the flow. After a little bit of algebra,

$$c \equiv \frac{\omega}{k} = \frac{\rho_1U_1+\rho_2U_2}{\rho_1+\rho_2} \pm \left[\frac{\left(\rho_2-\rho_1\right)g}{\left(\rho_2+\rho_1\right)k} - \frac{\left(\rho_1\rho_2\right)}{\left(\rho_2+\rho_1\right)^2}\left\{U_1-U_2\right\}^2\right]^{1/2} \qquad (11.1.12)$$

With the frequency determined we can easily find the structure of the wave by using the conditions (11.1.7 a, b). Of course, in this linear problem the over-all amplitude of the disturbance is arbitrary. But what we are interested in is the behavior in time and the x and z structure of the disturbance.

To gain insight in to the result (11.1.12) it is helpful to consider some special cases.

a) $U_1=U_2=0, \quad \dfrac{\rho_1}{\rho_2}\to 0$ **,**

The shear is set to zero and the upper layer has negligible density with respect to the lower layer so the system should mimic the simple gravity wave problem of Chapter 10. In fact (11.1.12) reduces to ;

$$\omega = \pm\left(gk\right)^{1/2} \qquad (11.1.13)$$

which is exactly the dispersion relation for a single layer in the short wave limit (short with respect to the depth) . See (10.4.34).

b) $U_1\neq 0, \quad U_2\neq 0, \ \dfrac{\rho_1}{\rho_2}\to 0$ **,**

Again, the density of the upper layer is negligible with respect to the lower layer so that even though there is now a shear across the interface there is no dynamical interaction of the two layers and the frequency is,

$$\omega = U_2 k \pm (gk)^{1/2} \qquad (11.1.14)$$

and the result is identical to the short wave (large depth) limit of (10.5.7), i.e. the gravity wave Doppler shifted by the mean current.

c) $U_1 = 0, U_2 = 0, \quad 0 < \rho_1 < \rho_2$ (11.1.15)

Still in the absence of shear across the interface, there is now a jump in density less than ρ_2 and the frequency is,

$$\omega = \pm \left[\left(\frac{\rho_2 - \rho_1}{\rho_2 + \rho_1} \right) gk \right]^{1/2} \qquad (11.1.16)$$

The *form* of the dispersion relation is exactly the same as for the single fluid model but, and this is true especially if the two densities are nearly equal, the frequency of the wave is much less than the single layer model since in that case ,

$$\left(\frac{\rho_2 - \rho_1}{\rho_2 + \rho_1} \right) g \equiv g' << g \qquad (11.1.17)$$

The frequency is reduced since gravity, g is replaced by g' which is called the *reduced gravity*. The free waves has relatively low frequencies with respect to the single layer model and the resulting motion seems to the observer beautifully sinuous. Returning to (11.1.7a), the velocity potentials in the two layers have opposite signs and so the x-velocity in the two layers will be equal and opposite and will be decaying away from the interface. Within a wavelength the motion will be exponentially small. If we considered a system with a free, upper surface as well as this interface, the motion due to these waves on the interface will tend to be limited to regions near the interface and be nearly unobservable at the surface. For that reason these waves are called *internal waves*.

If the two layers are shallow compared to a wavelength, the frequency of the internal wave is,

$$\omega = \pm k (g' D)^{1/2} \qquad (11.1.18)$$

In a famous experiment (Figure 11.1.2) , Ekman was able to explain the immense difficulty Norwegian, weakly powered , fishing boats had in making their way along narrow fjords in which the fresh surface water and the saltier ocean water combined to make a perfect environment for internal wave generation. When a vessel was moving at or near the velocity $(g'D)^{1/2}$ the propulsive energy of the ship was used to make internal waves instead of propelling the boat. It was locally called “dead water”. The locals knew they could solve the problem by moving at a different velocity but the explanation had to wait for the theory of internal gravity waves.

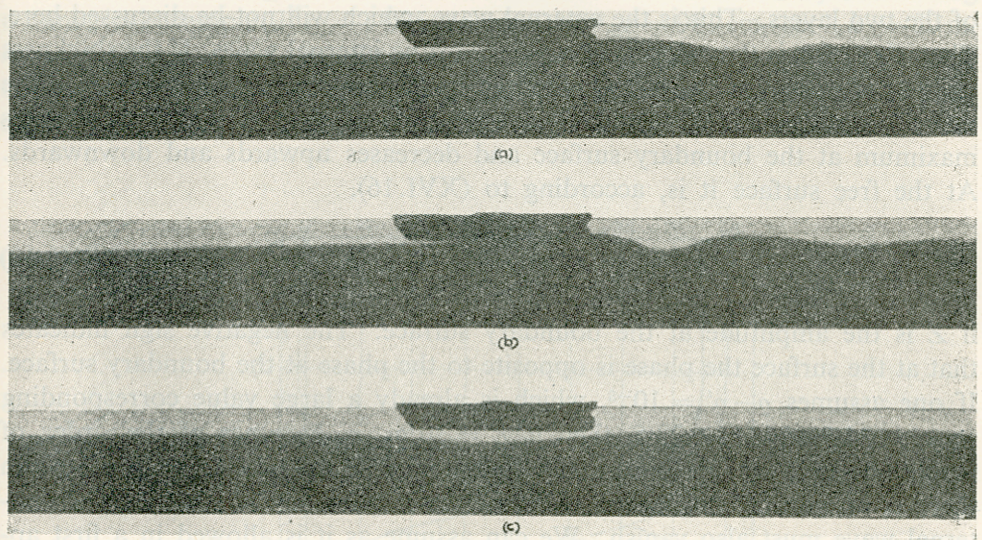

FIG. 214. Ekman's experiments on “dead water” waves. *a* and *b*, “dead water” waves created by a vessel; *c*, the ship is free from “dead water” waves.

Figure 11.1.2 A reproduction of Ekman’s experiment towing a model boat in a two - layer fresh/salty water system showing the production of internal gravity waves. The figure is from A. Defant, Physical Oceanography, vol. II Pergamon Press, 1961.

Note that if $\rho_1 > \rho_2$ the frequency becomes imaginary. Now, what does that mean? If $\rho_1 > \rho_2$

$$\omega = \pm i\sigma, \qquad \sigma = \left\{ \left(\frac{\rho_1 - \rho_2}{\rho_1 + \rho_2} \right) gk \right\}^{1/2} \tag{11.1.19}$$

and so the time dependence of the potential function becomes,

$$e^{-i\omega t} = e^{\pm\sigma t} \tag{11.1.20}$$

The root with the plus sign will yield *exponentially growing solutions in time*. This reflects the instability of the basic state that has heavy fluid on top of light fluid. A small disturbance will immediately cause the interface to explode in a series of plumes of sinking heavy water and rising lighter water. Note that the growth rate, σ, is larger for larger k, i.e. for shorter waves, leading to narrow regions of rising and sinking motion. This is the fundamental region why cumulus clouds are so narrow in the atmosphere. Of course, when the scale gets very small both friction and thermal diffusion become important and the full theory of thermal convection informs us that a certain density difference is required to overcome the loss of energy experienced by the plumes before convection can occur but a discussion of this interesting subject is beyond the scope of this introductory course.

d) $U_1 \neq U_2, \qquad \rho_1 = \rho_2$

In this example the is no density variation in the fluid but the velocities of the mean flow are different in each layer and so now,

$$\sigma = \frac{U_1 + U_2}{2}k \pm i\frac{|U_1 - U_2|}{2}k \tag{11.1.21}$$

The first term on the right hand side of (11.1.21) is just the Doppler shift of the frequency by an amount that depends on the average of the velocities of the two streams. The second term is more interesting. It always yields an imaginary contribution to the frequency and the corresponding growth rate is larger the small the wavelength o f the disturbance. This a *shear instability* and is also called a *Helmholtz instability*, named for the great German physicist who first studied it. Strong shears will give rise to these small scale instabilities and they are the fundamental mechanism for small scale turbulence in the atmosphere and the oceans. The general argument for a continuous profile of velocity is as follows:

Consider a flow in the x direction, as shown in Figure 11.1.3. For definiteness let's suppose is rests between two horizontal plates and, for the moment, let's ignore friction.

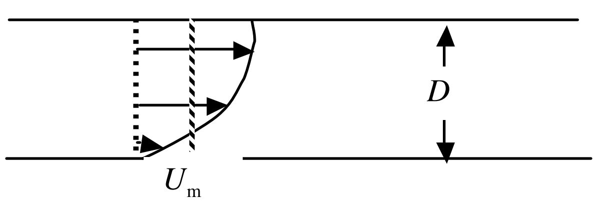

Figure 11.1.3 A velocity profile *U(z)* showing the mean velocity U_m as the textured line.

If the vertical extent of the region is D then the total momentum for the flow in the ex direction is (assuming constant density)

$$M = \rho \int_0^D u dz = \rho D U_m \qquad (11.1.22)$$

Since there is no friction to be considered this total momentum of the flow must be conserved since there is no net force acting in the x direction to change it. Now consider the total energy of the flow whose general velocity is,

$$u = U_m + u' \qquad (11.1.23)$$

The kinetic energy is,

$$\frac{1}{2}\int_0^D \rho u^2 dz = \frac{1}{2}\int_0^D \rho \left(U_m + u'\right)^2 dz = \frac{1}{2}\int_0^D \rho \left[U_m{}^2 + 2U_m u' + u'^2\right] dz \qquad (11.1.24)$$

$$\frac{1}{2}\rho D U_m{}^2 + \frac{1}{2}\rho \int_0^D u'^2 dz$$

so that the mean flow possesses the minimum energy consistent with the conservation of momentum when its velocity profile coincides with the uniform flow U_m. Any disturbance that can smooth the velocity profile and reduce its departure from the mean will reduce the energy in the mean flow and since total energy is conserved that energy is then available for eddying, turbulent motion. For a given mean flow, the stronger the shear the more energy is available to feed the instability and produce growth of the perturbation and subsequent turbulence.

The mechanism for the original growth of the disturbance is as follows: Consider the interface as it begins to deform as shown in Figure 11.1.4.

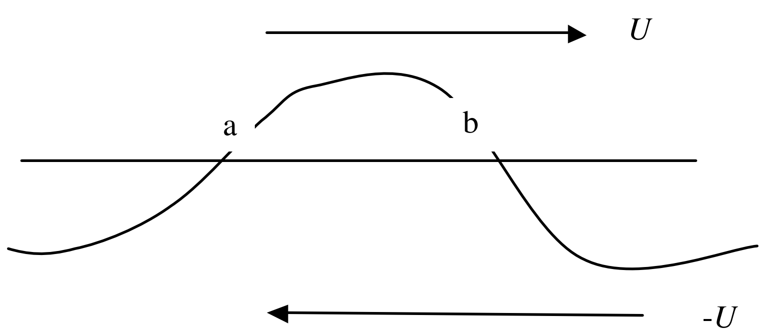

Figure 11.1.5 The schematic to discuss the pressure distribution on the interface

Let us move with the average of the velocities so the mean flow is equal and opposite in the two layers. The wave is not propagating in this frame. As the interface is deformed the flow speeds up over the crest of the wave (much like the flow around the cylinder studied in section 10.3. Since $\partial u / \partial t > 0$ there that means the pressure gradient will be negative at the crest since,

$$u_t + uu_x = -\frac{p_x}{\rho} \qquad (11.1.25)$$

and u_x is zero at the crest by symmetry. That also implies that upstream of the crest, at the point a in the figure, the pressure will be higher than at point b. So the mean flow will be doing work on the rippled interface delivering energy to the disturbance and this accounts for its growth. You should check that the same argument works in the lower layer.

Just as for the case when the densities destabilized the system we must not take the prediction of ever increasing growth rate with increasing *k* seriously. For large *k* friction will be important but more important yet is that as the scale of the wave shrinks the idealization of the shear layer as being infinitely sharp becomes unrealistic. For continuous shear profiles, even sharp ones there is usually a wavenumber beyond which disturbances are stable.

e) $U_1 \neq U_2, \qquad \rho_2 > \rho_1$

This is the general case and we are prepared for the nature of the result. The density structure is stable and by itself will support stable internal waves due to the gravitational restoring force that occurs when heavy fluid is lifted into lighter fluid. On the other hand the shear will act to destabilize the flow. According to 11.1.12 instability, called *Kelvin-Helmholtz Instability* will occur whenever the radicand in that equation becomes negative or whenever the shear is strong enough i.e.,

$$\frac{(\rho_2 - \rho_1)g}{(\rho_2 + \rho_1)k} < \frac{(\rho_1 \rho_2)}{(\rho_2 + \rho_1)^2}\{U_1 - U_2\}^2 \qquad (11.1.26)$$

Note that the condition is scale dependent. According to (11.1.26) short enough waves will always be unstable. This is a flaw in the model as noted earlier. For very small wavelength the detailed structure of the shear zone can't be ignored and when the wavelength is of the same order as the width of the shear zone the buoyancy forces can stabilize the shear layer.

These disturbances are often visible in the sky as rolling billow waves. Some years ago John Woods (J. Fluid Mech. 1968 vol 32pp 791-800) photographed the phenomenon on a shallow thermocline in the Mediterranean and his beautiful photos are shown in Figure 11.1.6.

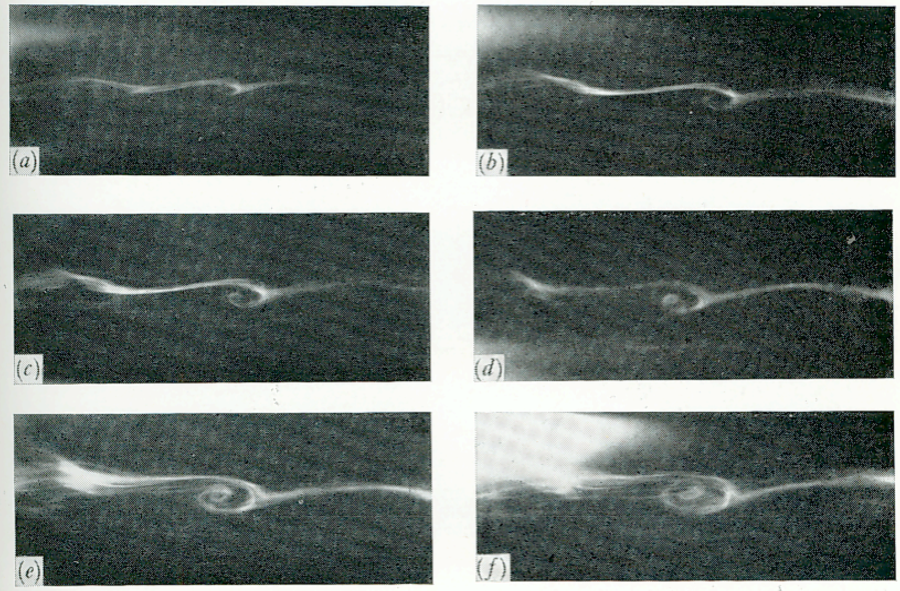

Fig. 4.20. Stages in the development of a billow produced by a long wave travelling along an interface in the thermocline. (From Woods 1968*b*.)

11.2 The Richardson number

We can generalize the condition (11.1.26) thanks to a beautiful theorem proved by L.N. Howard , 1961, J. Fluid Mech. **10**,509-512 which clarified an earlier but more complex proof by John Miles (same issue of the journal). But first let us consider what the qualitative condition, in general, might be. Over a region δz the amount of kinetic energy available for transformation into perturbations (11.1.24) will be of the order of

$$\rho \Delta U^2 \approx \rho \left(\frac{dU}{dz} \delta z \right)^2 \qquad (11.2.1)$$

while the energy expended by raising a fluid element in a background stratification is the buoyancy restoring force times the distance moved, $\Delta\rho g\delta z$. But since $\Delta\rho \approx \frac{d\rho}{dz}\delta z$, the energy used to fight the stable stratification is,

$$\Delta\rho g\delta z = -\frac{d\rho}{dz} g(\delta z)^2 \qquad (11.2.2)$$

so that the ratio of the energy available to drive the instability compared to the energy used up in fighting the stabilizing effect of buoyancy is the ratio of these two expressions. Traditionally, the ratio is measured the other way around, i.e. the ratio of the energy expended against gravity with respect tot he shear energy available to drive the instability is,

$$R_i = \frac{-g\frac{d\rho}{dz}}{\rho\left(\frac{dU}{dz}\right)^2} \qquad (11.2.3)$$

This non dimensional parameter is called the *Richardson number*. For a stratified fluid, as we defined it in section 9.3 the buoyancy frequency N is

$$N = \left(\frac{-g}{\rho}\frac{d\rho}{dz}\right)^{1/2} \qquad (11.2.4)$$

so that the Richardson number is

$$\boxed{R_i = \frac{N^2}{U_z^{\,2}}} \qquad (11.2.5)$$

For an atmospheric flow the buoyancy frequency is defined in terms of the potential temperature, θ, so that

$$N = \left(\frac{g}{\theta}\frac{\partial\theta}{\partial z}\right)^{1/2} \qquad (11.2.6)$$

And from simple physical reasoning we can expect that the condition for instability will be that R_i must be less than some critical value for instability. We shall show, following Howard's proof , that *the critical value is exactly 0.25.*

Consider a mean flow in the x direction *U(z)* and suppose we add a small perturbation, (u',w') to the velocity. We will also assume for simplicity that the density field is composed of a mean density ρ_s (z) and a perturbation $\rho'(x,z,t)$ and similarly for the pressure. Furthermore, as in the oceanic case the mean density is very nearly equal to its average ρ_0 so that in the horizontal acceleration terms the density can be replaced by this constant value, i.e. the *Boussinesq approximation*. Our linearized equations of motion, ignoring friction and assuming the scale is small enough to ignore the effect of planetary rotation is:,

$$\rho_0\left(u'_t + Uu'_x + w'U_z\right) = -\frac{\partial p'}{\partial x},$$

$$\rho_o(w'_t + Uw'_x \qquad) = -\frac{\partial p'}{\partial z} - \rho' g, \tag{11.2.7 a, b, c, d}$$

$$u'_x + w'_z = 0,$$

$$\left(\rho'_t + U\rho'_x\right) + w'\frac{\partial \rho_s}{\partial z} = 0.$$

Cross differentiating the first two equation in x and z to eliminate the pressure yields an equation for the y component of the vorticity, $\eta = \frac{\partial u'}{\partial z} - \frac{\partial w'}{\partial x}$,

$$\left[\frac{\partial}{\partial t} + U\frac{\partial}{\partial x}\right]\eta + w'U_{zz} = g\frac{\rho'_x}{\rho_0} \tag{11.2.8}$$

We define the differential operator,

$$D = \left(\frac{\partial}{\partial t} + U\frac{\partial}{\partial x}\right) \tag{11.2.9}$$

so that (11.2.8) and (11.2.7 d) are ,

$$D\eta + w'U_{zz} = g\frac{\rho'_x}{\rho_s}, \qquad \text{(11.2.10 a , b)}$$
$$D\rho' + w'\rho_{s_z} = 0.$$

and using (11.2.10 b) to eliminate the density perturbation from (11.2.10 a) we obtain,

$$D^2\eta + Dw'U_{zz} = \frac{g}{\rho_0}\frac{\partial}{\partial x}D\rho' = -\frac{g}{\rho_0}\frac{\partial}{\partial x}w'\rho_{s_z} = N^2\frac{\partial w'}{\partial x} \quad (11.2.11)$$

Since the motion is two dimensional and incompressible (but *not* irrotational) we can introduce a stream function,

$$u = -\psi_z, \quad w = \psi_x \quad (11.2.12)$$

so that ,

$$\eta = -\nabla^2\psi \quad (11.2.13)$$

allowing us to write (11.2.11) entirely in terms of ψ ,

$$D^2\nabla^2\psi - U_{zz}D\psi + N^2\frac{\partial^2\psi}{\partial x^2} = 0 \quad (11.2.14)$$

This equation is sometimes called the *Taylor-Goldstein* equation and has been studied for many particular velocity profiles *U(z)* and in many case detailed calculations have indicated that the Richardson number, that is the ratio N^2/U_z^2 had to be somewhere in the flow less than 1/4 for instability to arise. Many people felt that there had to be some universal criterion of that type but it was not until John Miles presented his proof that it was successfully derived. Miles' proof is rather complex and accompanied with restrictions on the analytic nature of *N* and *U*. Howard, in reviewing the paper found a much simpler proof which we present here.

We look for solutions of (11.2.14) in the form,

$$\psi = \phi e^{ik[x-ct]} \quad (11.2.15)$$

where it is the real part of the expression that is implied. The boundary conditions at the horizontal boundaries, say at z=0 and z=*H* are that *w'* =0. That implies that ϕ is zero at those boundaries. Using (11.2.15) in (11.2.14) yields,

$$(U-c)^2\left[\phi_{zz}-k^2\phi\right]+\phi\left[N^2-U_{zz}(U-c)\right]=0,$$

(11.2.16 a, b)

$$\phi=0, \qquad z=0,H$$

Howard suggested introducing the function ,

$$G=\frac{\phi}{(U-c)^{1/2}} \qquad (11.2.17)$$

in terms of which,

$$\phi_z=G_z(U-c)^{1/2}+\frac{1}{2}U_z\frac{G}{(U-c)^{1/2}},$$

(11.2.18 a,b)

$$\phi_{zz}=G_{zz}(U-c)^{1/2}+\frac{G_zU_z}{(U-c)^{1/2}}+\frac{1}{2}\frac{U_{zz}G}{(U-c)^{1/2}}-\frac{1}{4}\frac{U_z^{\,2}}{(U-c)^{3/2}}G$$

The governing equation for ϕ then becomes the following equation for G,

$$\frac{d}{dz}(U-c)\frac{dG}{dz}-\left[\frac{1}{2}U_{zz}+k^2(U-c)\right]G+\left[N^2-\frac{U_z^{\,2}}{4}\right]\frac{G}{(U-c)}=0 \quad (11.2.19)$$

with boundary conditions G_z=0, z=0 , H. We can think of (11.1.19) as an *eigenvalue* problem for the phase speed c for a given k. If c has an imaginary part greater than zero the flow will be unstable. Note that since (11.2.19) has real coefficients if G is a solution with an eigenvalue c then G^* (the complex conjugate) will also be a solution with eigenvalue c^*, a result easily obtained by taking the complex conjugate of (11.2.19). Thus a condition for instability is simply that (11.2.19) have a solution with a complex c.

As in the usual eigenvalue problems we obtain useful information about the eigenvalue by multiplying the equation by the complex conjugate of the eigenfunction and integrating over the interval (0,H). We note that,

$$\int_0^H G^*\frac{d}{dz}\left[(U-c)\frac{dG}{dz}\right]dz=\cancelto{0}{G^*(U-c)\frac{dG}{dz}\Big]_0^H}-\int_0^H\left|\frac{dG}{dz}\right|^2(U-c)\,dz \qquad (11.2.20)$$

and the first term on the right hand side vanishes since G and its complex conjugate vanish at the end points. The resulting integral of the equation is,

$$-\int_0^H (U-c)\left[\left|\frac{dG}{dz}\right|^2 + k^2|G|^2\right]dz - \frac{1}{2}\int_0^H |G|^2 U_{zz}dz + \int_0^H \frac{|G|^2}{(U-c)}\left[N^2 - \frac{1}{4}U_z^{\,2}\right]dz = 0 \quad (11.2.21)$$

In the factor of the last term on the left hand side we write,

$$\frac{|G|^2}{(U-c)} = \frac{|G|^2(U-c^*)}{|U-c|^2} \qquad (11.2.22)$$

Our final step is to take the imaginary part of (11.2.21) using (11.2.22). Only the first and third terms in (11.2.21) contribute and each in proportional to c_i the imaginary part of *c*. We obtain,

$$c_i\left[\int_0^H \left(|G_z|^2 + k^2|G|^2\right)dz + \int_0^H \frac{|G|^2}{|U-c|^2}\left[N^2 - \frac{U_z^{\,2}}{4}\right]dz\right] = 0 \qquad (11.2.23)$$

For instability we must have c_i different from zero. This means the sum of the two integrals in the square brackets of (11.2.23) must vanish. However, the first integral is always positive. Therefore if, in the second integral, $N^2 > \frac{1}{4}U_z^{\,2}$ everywhere in the flow c_i would have to be zero and the flow would be stable to small perturbations. Therefore, a *necessary condition* for instability is that, at least somewhere in the flow, the Richardson number must be less than 1/4. In fact in many cases studied this necessary condition turns out to be sufficient. Observations have also confirmed the pertinence of the criterion. Eriksen (J.G.R, 1978, vol. 83 2989-3009) examined long term measurements of breaking internal gravity waves near Bermuda and presented a scatter plot of the measured shear and buoyancy frequency when wave breaking turbulence was observed. His scatter plot is shown below in Figure 11.2.1. The straight line in the figure is the line R_i =1/4 and it is clear that the Richardson number accompanying most of the observations of wave breaking were in the range less than 1/4 (note the inversion of the axes) Similar observations in the atmosphere have reached similar results, at least qualitatively.

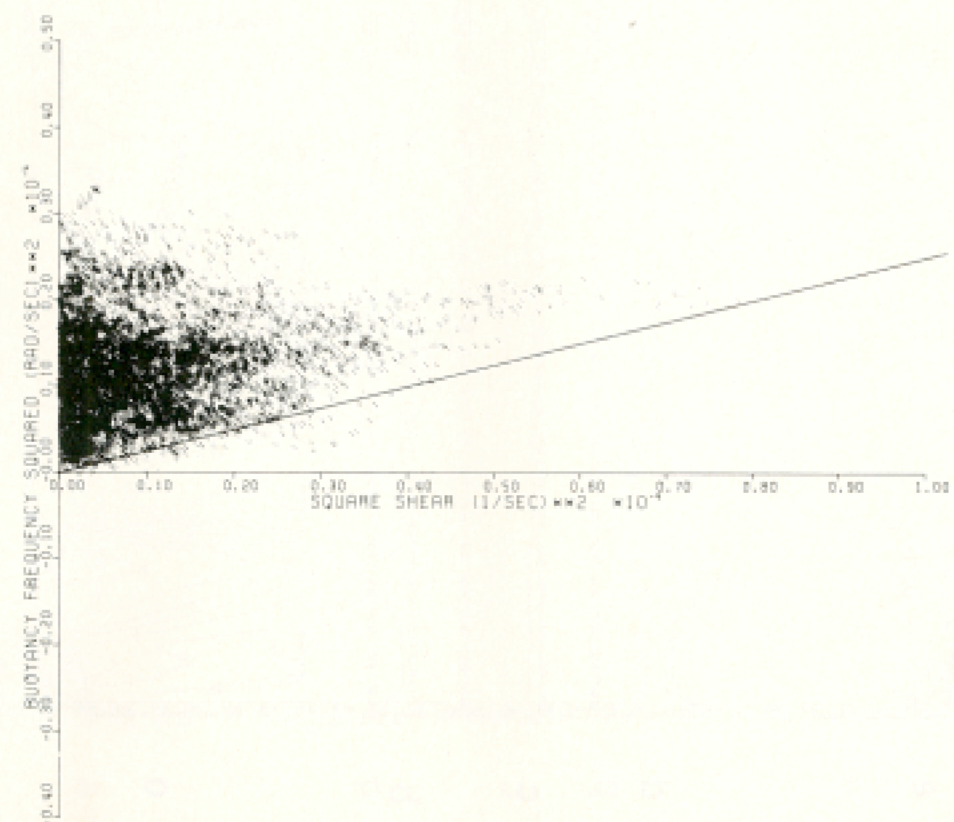

Fig. 20. Scatter plot of shear squared over 6.3 m versus N^2 (7.13 m) of estimates made every 40 s during a 78-hour segment of the second experiment. Of the 7020 points the 6881 with acceptable quality at both the upper and lower cluster on the forward mast are plotted. The line corresponds to Ri = 0.25.

Figure 11.2.1 A scatter plot of showing the location of observations in U_z ,N space where internal gravity wave breaking is observed (from Eriksen , 1978)

11.3 Baroclinic Instability

Another type of instability also involving shear and buoyancy effects occurs on much larger scales in both the atmosphere and the oceans for which the Earth's rotation is crucial for the existence of the instability. This is the so-called *baroclinic instability*. The essence of the phenomenon can be qualitatively understood by considering the thermal wind and hydrostatic equations. Again, for simplicity we well use the dynamics of an incompressible fluid but the discussion for the atmosphere is nearly identical with potential temperature taking the place of the density.

As we have seen, the thermal wind equations for an incompressible fluid yield, in the zonal (i.e. x) direction, (see eqn. 9.2.25)

$$\rho_0 f \frac{\partial u}{\partial z} = g\frac{\partial \rho}{\partial y},$$

$$N^2 = -\frac{g}{\rho_0}\frac{\partial \rho}{\partial z} \qquad \text{(11.3.1 a, b)}$$

so that the slope of the density surfaces in the y.z plane is,

$$\left.\frac{\partial z}{\partial y}\right)_{\rho} = -\frac{\dfrac{\partial \rho}{\partial y}}{\dfrac{\partial \rho}{\partial z}} = \frac{f\dfrac{\partial u}{\partial z}}{N^2} \qquad \text{(11.3.2)}$$

as shown in Figure 11.3.1

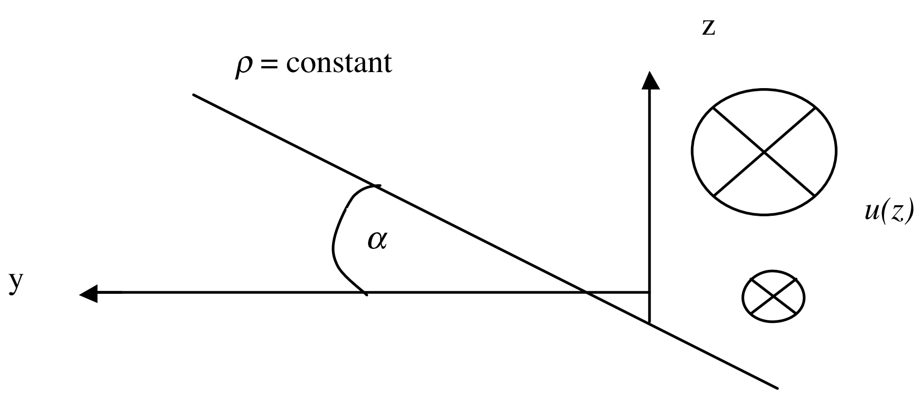

Figure 11.3.1 The slope of the density surfaces in the presence of a zonal (x) velocity increasing in z.

The slope is generally small, in the oceanic case in mid-latitudes it is not larger than 10^{-3} but the slope is nevertheless dynamically significant. Consider the virtual (i.e. imagined) displacement of the fluid elements shown in Figure 11.3.2.

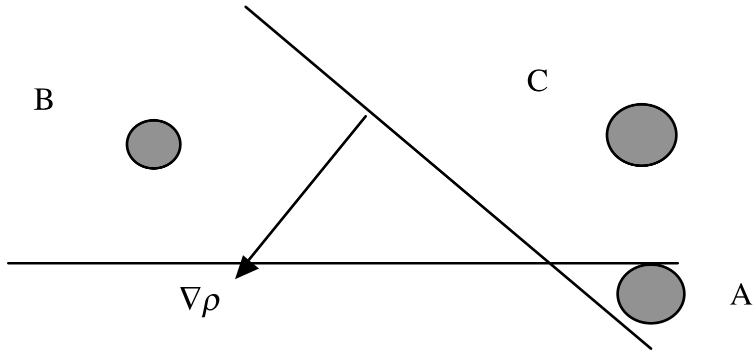

Figure 11.3.3 The position of three fluid elements in position before virtual displacements. The direction of the density gradient is also shown.

Element A is below both the elements B and C. Element C is directly above element A and in an ocean (or atmosphere) stably stratified it will be lighter than element A. If we imagine A lifted slowly to the position of C, the element A would be heavier than C and would tend to sink back down towards its original position due to a gravitational restoring force. On the other hand, with the sloping density surfaces as shown in the figure, element A is *lighter* than element B even though B is higher than element A i.e. at a geopotential surface above it. Thus, if we imagine A moved to the position of B, it will arrive at B and be lighter than the surrounding fluid and so the buoyancy force acting on it will actually tend to encourage a further motion along that direction.

To calculated the force on the displaced element A at point B we need only calculate the Archimedean buoyancy force per unit mass as,

$$
\begin{aligned}
F_g &= g\frac{\delta\rho}{\rho_0} = g\frac{\rho_A - \rho_B}{\rho_0} \\
&\approx \frac{g}{\rho_0}\left[\rho_A - \left(\rho_A + \frac{\partial\rho}{\partial z}\delta z + \frac{\partial\rho}{\partial y}\delta y + \ldots\right)\right]
\end{aligned}
\tag{11.3.3}
$$

assuming the original positions of A and B are close enough for a Taylor Series expansion to provide us with an estimate of the density difference, Thus the vertical buoyancy force per unit mass is,

$$
F_g = -\frac{g}{\rho_o}\left(\frac{\partial\rho}{\partial z}\delta z + \frac{\partial\rho}{\partial y}\delta y\right) \tag{11.3.4}
$$

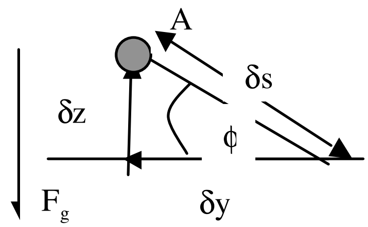

Figure 11.3.4 The displacement of fluid element A at an angle ϕ with respect to the horizontal where $\tan\phi = \dfrac{\delta z}{\delta y}$ and δs is the distance of the displacement.

The component of the gravitational force along the displacement path, measured positive in the direction of the displacement is

$$
\begin{aligned}
-F_g \sin\phi &= \frac{g}{\rho_o}\frac{\partial\rho}{\partial z}\delta z\left[1+\frac{\rho_y/\rho_z}{\delta z/\delta y}\right]\sin\phi \\
&= -N^2\delta s\left[1-\frac{\left(\dfrac{\partial z}{\partial y}\right)_\rho}{\tan\phi}\right]\sin^2\phi \qquad (11.3.5) \\
&= -N^2\delta s\left[1-\frac{\tan\alpha}{\tan\phi}\right]\sin^2\phi
\end{aligned}
$$

Now consider different displacements. If A is moved to the position of C, δy is zero and the force in the direction of the displacement is just $-N^2\delta s$ and we recognize this as the restoring "spring constant" force of a mass spring oscillator whose natural frequency is *N*. Indeed, this is why *N* is called the buoyancy frequency. The restoring force is positive as long as *N* is real representing a stable stratification. If, on the other hand, the displacement is made such that $\phi < \alpha$, i.e. the displacement lies within the wedge opened up by the sloping density surfaces, then the force in the direction of the displacement will be positive, not restoring at all, but instead will push the element further from its original position. Thus we anticipate that fluid displacements that take place in the wedge between the horizontal (i.e. the geopotential) and the sloping density surface as shown in Figure

11.3.1, will release energy and that the result will be an instability of the original zonal flow. The resulting instability is called baroclinic instability because the source of the instability is the sloping density surfaces and the instability can be shown to manifest itself as a growing wave which in the atmosphere can be identified as a synoptic scale weather disturbance and in the ocean in the form of mid-ocean eddies.

We can estimate the characteristic scale of the disturbance as follows:
For instability,

$$\frac{\delta z}{\delta y} = \frac{w}{v} < \tan\alpha = \frac{fU_z}{N^2} \tag{11. 3.6}$$

We need to make an estimate of the ratio of the vertical to horizontal velocity. If D is the vertical scale of the motion and L is the vertical scale of the motion then from geometrical arguments and the constraint of the continuity equation we might imagine that a good estimate of w/v would be D/L. However, we also noted in section 9.2 that if the motion was in quasi-geostrophic balance the horizontal velocity would be non divergent to lowest order and the continuity equation at that order will not produce a vertical velocity. On the synoptic scale the vertical velocity is produced by the departures from geostrophy. We can use the vorticity equation for the vertical component of vorticity to estimate w. To lowest order in Rossby number,

$$\frac{d\zeta}{dt} + \beta v = f_o \frac{\partial w}{\partial z} \tag{11.3.7}$$

where $\zeta = v_x - u_y$. If U is a characteristic horizontal velocity, the first term on the left hand side is of order,

$$\frac{d\zeta}{dt} = O(\frac{U^2}{L^2}) \tag{11.3.8}$$

and if this is balanced by the stretching term on the right hand side which is order $f_o \, {}^{w}\!/\!_{D}$ our estimate for the ratio, w/v would be,

$$\frac{w}{v} = O\left(\frac{w}{U}\right) = O\left(\frac{U^2}{Uf_oL}\frac{D}{L}\right) = R_o\frac{D}{L} \tag{11.3.9}$$

and using (11.3.6) we obtain,

$$\frac{w}{v} \sim \frac{UD}{f_0 L^2} < \frac{f_o U_z}{N^2} \approx \frac{f_0 U}{N^2 D} \tag{11.3.10}$$

or for instability the requirement is that the horizontal scale of the perturbation satisfy,

$$L^2 > \frac{N^2 D^2}{f_o^{\,2}} \tag{11.3.11}$$

or that L exceed the *Rossby deformation radius* ND/f_0. Detailed calculations show that the maximum growth rate occurs when the scale of the perturbation is of the order of the deformation radius but somewhat larger. This leads to scales of the order of 500 km for the atmosphere and 50 km for the oceans and this is precisely the synoptic scale in both fluids.

We can make an educated guess about the growth rates as follows. As in section 11.1 the growth rate will be the imaginary part of the phase speed of the disturbance and we can imagine that the phase speed will be of the order of the flow in which the disturbance is embedded. If the disturbance went much faster than the flow it would not “see” the shear, the fluid would appear to be essentially at rest and we would not expect instability in such a case. We therefore anticipate that,

$$\mathrm{Im}(c) \approx U \approx U_z D \tag{11.3.12}$$

In fact, there is a theorem, originally due to Howard (same reference as for the Richardson number proof) that supports this heuristic reasoning. The frequency is the wavenumber times the phase speed and the wavenumber is essentially the inverse of the characteristic length of the disturbance and we have already noted that the length will be of the order of the deformation radius. We therefore anticipate a growth rate,

$$\sigma = \frac{c_i}{L} \approx \frac{U_z D}{ND / f_o} = \frac{f_o}{N} U_z \tag{11.3.13}$$

also confirmed by detailed calculations (see GFD chapter 7).